Open Access Library Journal
2026, Volume 13, e16042
ISSN Online: 2333-9721
ISSN Print: 2333-9705

A Simple Geometric Equation That Generates a Wide Variety of Geometric Shapes and Forms

Salomon Mboninyibuka[1], Hippolyte Nyengeri[2]

[1]Department of Informatics, Ministry of Finance, Budget and Digital Economy, Bujumbura, Burundi
[2]Department of Physics, University of Burundi, Bujumbura, Burundi
Email: hippolyte.nyengeri@ub.edu.bi

How to cite this paper: Mboninyibuka, S. and Nyengeri, H. (2026) A Simple Geometric Equation That Generates a Wide Variety of Geometric Shapes and Forms. *Open Access Library Journal*, **13**: e16042.
https://doi.org/10.4236/oalib.1116042

Received: September 17, 2026
Accepted: November 13, 2026
Published: November 16, 2026

Copyright © 2026 by author(s) and Open Access Library Inc.
This work is licensed under the Creative Commons Attribution International License (CC BY 4.0).
http://creativecommons.org/licenses/by/4.0/
Open Access

Abstract

In this paper, we develop a new geometrical approach that can be used to describe many geometrical shapes and forms. Starting from the equation of the unit rhombus, we show that a large variety of shapes can be obtained using a single and simple geometrical equation, together with two basic 2-dimensional geometric transformations. We also show that applying the polar equation to some functions modifies the behavior of these functions and then the shapes of the associated graphs.

Subject Areas

Geometry

Keywords

Unit Rhombus, Cartesian Equation, Polar Equation, Non-Linear Scaling, Roration

1. Introduction

Form in plants and other organisms has intrigued students of nature for a long time [1] [2]. With the advent of computer technology, various methods of synthesizing and analyzing patterns (e.g., images and waveforms, such as sounds and various electromagnetic waveforms including light, electricity, etc.) have been developed [1] [2].

While variation in form and shape has always intrigued students of nature (e.g., such as biologists and mathematicians), creating accurate and simple characterization of form and shape has proven to be conceptually arduous task. There remains a need for simple mathematical and biophysical rules underlying shapes in

general and morphology and morphogenesis.

The ancient Greeks developed some basic geometric principles to explain natural forms. In both ancient and modern concepts, the circle prevails as the ideal object. Generally, circular and cylindrical forms and shapes can also be observed in plants and organisms. Much of existing geometry is based on the circle, including all trigonometry and all technology based on trigonometric functions. Complex forms can also be analyzed in terms of circles and harmonics.

More recently, other findings to describe natural forms have included, for example, fractals and algorithms that can, for example, generate some types of virtual plants. Besides, a geometrical approach based on the use of the so-called superellipse equation given by [3]-[8]

$$\left|\frac{x}{a}\right|^n + \left|\frac{y}{b}\right|^n = 1 \tag{1}$$

where n, a and b are positive numbers, and the vertical bars around a number indicate the absolute value of the number, has been developed. This curve was analyzed for the first time in 1818 by the French mathematician Gabriel Lamé [9]. Therefore it is called a *Lamé curve* [7]. On the other hand, in the middle of the 20th century, the Danish scientist and artist Piet Hein suggested a Lamé curve, which he called a *superellipse*, for the roundabout at Sergels torg (Sergel's Square) in central Stockholm [6]-[9]. Since then, Lamé curves (superellipses) have become one of the symbols of Scandinavian design.

Let us emphasize that in the polar coordinate system, the superellipse equation is (the set of all points (ρ,θ) on the curve satisfying the equation):

$$\rho(\theta) = \left(\left|\frac{\cos\theta}{a}\right|^n + \left|\frac{\sin\theta}{b}\right|^n\right)^{-1/n}. \tag{2}$$

We have to add that Equation (2) has been generalized as follows [1] [2]:

$$\rho(\theta) = \frac{1}{\sqrt[n_1]{\left|\frac{1}{a}\cos\left(\frac{m_1\theta}{4}\right)\right|^{n_2} \pm \left|\frac{1}{b}\sin\left(\frac{m_2\theta}{4}\right)\right|^{n_3}}}. \tag{3}$$

Equation (3) is known as *super-formula*. It permits generation of very wide range of natural and abstract shapes [1] [2], but it seems to be complex since too many parameters are involved in it.

The main purpose of our work is to develop a new geometrical approach that can be used to describe many geometrical shapes and forms from a very simple mathematical formula and basic 2-dimensional geometric transformations.

The paper is organized as follows. In Section 2, we present the cartesian and polar forms for the mathematical formula to be considered. We also show how to increase its degree of freedom with the aid of two of the basic 2-dimensional geometric transformations (scaling and rotation). In Section 3, we present and comment shapes and forms that may be obtained from our approach. The conclusion is given in Section 4.

2. Materials and Methods

At an initial stage, the equation for a unit rhombus in cartesian coordinates is presented.

$$|x|+|y|=1. \tag{4}$$

The main desadvantage of this equation is that it has any degree of freedom and then can generate only one geometric form, *i.e.*, the unit rhombus.

By adding a non-linear term of type $\sigma\sqrt{|x||y|}$ in the left-hand side of Equation (4), with $-2<\sigma<+\infty$, which gives the expression

$$|x|+|y|+\sigma\sqrt{|x||y|}=1, \tag{5}$$

it is possible to generate many geometrical shapes and forms as shown in **Figures 1-4**.

Note that Equation (5) can be transformed into polar coordinates by substituting the relations

$$x=\rho\cos\theta \tag{6}$$

and

$$y=\rho\sin\theta \tag{7}$$

which express the cartesian coordinates x and y in terms of polar coordinates ρ and θ, into this equation, which yields

$$\rho\left(|\cos\theta|+|\sin\theta|+\sigma\sqrt{|\cos\theta||\sin\theta|}\right)=1 \tag{8}$$

or

$$\rho(\theta)=\frac{1}{|\cos\theta|+|\sin\theta|+\sigma\sqrt{|\cos\theta||\sin\theta|}} \tag{9}$$

In addition, further shape moderation can be accomplished by introducing differences in axis length with the aid of non-linear scaling such that

$$\begin{pmatrix}x\\y\end{pmatrix}\mapsto\begin{pmatrix}1/a & 0\\0 & 1/b\end{pmatrix}\begin{pmatrix}x\\y\end{pmatrix} \tag{10}$$

where a and b are positive numbers. After this transformation, Equation (5) becomes

$$\left|\frac{x}{a}\right|+\left|\frac{y}{b}\right|+\sigma\sqrt{\left|\frac{x}{a}\right|\left|\frac{y}{b}\right|}=1, \tag{11}$$

and the polar equation (9) becomes

$$\rho(\theta)=\frac{1}{\left|\frac{\cos\theta}{a}\right|+\left|\frac{\sin\theta}{b}\right|+\sigma\sqrt{\left|\frac{\cos\theta}{a}\right|\left|\frac{\sin\theta}{b}\right|}} \tag{12}$$

Another transformation of Equation (5) which may enables moderation of shapes is rotation of a certain angle ϕ with respect to the origin, which yields

$$\begin{aligned}&|\cos(\phi)x-\sin(\phi)y|+|\sin(\phi)x+\cos(\phi)y|\\&+\sigma\sqrt{|\cos(\phi)x-\sin(\phi)y||\sin(\phi)x+\cos(\phi)y|}=1\end{aligned} \tag{13}$$

for the cartesian equation and

$$\rho(\theta)=\frac{1}{\left|\cos(\phi+\theta)\right|+\left|\sin(\phi+\theta)\right|+\sigma\sqrt{\left|\cos(\phi+\theta)\right|\left|\sin(\phi+\theta)\right|}} \tag{14}$$

for the polar one.

In the particular case when $\phi=\pi/4$, Equation (13) and (14) give

$$|x-y|+|x+y|+\sigma\sqrt{|x-y||x+y|}=\sqrt{2} \tag{15}$$

and

$$\rho(\theta)=\frac{\sqrt{2}}{\left|\cos\theta-\sin\theta\right|+\left|\cos\theta+\sin\theta\right|+\sigma\sqrt{\left|\cos\theta-\sin\theta\right|\left|\cos\theta+\sin\theta\right|}} \tag{16}$$

respectively. If this rotation is only applied to the last term of the left-hand side of Equation (5), we obtain

$$|x|+|y|+\frac{\sigma}{\sqrt{2}}\sqrt{|x-y||x+y|}=1 \tag{17}$$

for the cartesian equation and

$$\rho(\theta)=\frac{1}{\left|\cos\theta\right|+\left|\sin\theta\right|+\frac{\sigma}{\sqrt{2}}\sqrt{\left|\cos\theta-\sin\theta\right|\left|\cos\theta+\sin\theta\right|}} \tag{18}$$

for the polar one.

Note that when our initial cartesian Equation (5) is subject to both a scaling transformation and a rotation, we obtain the following expression

$$\begin{aligned}&\left|\cos(\phi)\frac{x}{a}-\sin(\phi)\frac{y}{b}\right|+\left|\sin(\phi)\frac{x}{a}+\cos(\phi)\frac{y}{b}\right|\\&+\sigma\sqrt{\left|\cos(\phi)\frac{x}{a}-\sin(\phi)\frac{y}{b}\right|\left|\sin(\phi)\frac{x}{a}+\cos(\phi)\frac{y}{b}\right|}=1.\end{aligned} \tag{19}$$

In this case, the polar equation is

$$\rho(\theta)=1/f(a,b,\sigma,\theta,\phi) \tag{20}$$

where

$$\begin{aligned}f(a,b,\sigma,\theta,\phi)=&\left|\cos\phi\frac{\cos\theta}{a}-\sin\phi\frac{\sin\theta}{b}\right|+\left|\sin\phi\frac{\cos\theta}{a}+\cos\phi\frac{\sin\theta}{b}\right|\\&+\sigma\sqrt{\left|\cos\phi\frac{\cos\theta}{a}-\sin\phi\frac{\sin\theta}{b}\right|\left|\sin\phi\frac{\cos\theta}{a}+\cos\phi\frac{\sin\theta}{b}\right|}\end{aligned} \tag{21}$$

Before finishing this section, we have to indicate that new geometrical shapes and forms can be generated by considering trigonometric functions (cosine and sine functions) resulting from the generalization of the familiar trigonometry (circular trigonometry) to our equation, or by adding or multiplying side by side two distinct equations obtained from (19) by choosing two different sets of parameters.

The novelty of our family of curves lies in that it is easily obtained from a very simple geometric equation (with only one degree of freedom), together with two well-known basic 2-dimensional geometric transformations. This doesn't prevent him from

describing a lot of shapes. Some of these shapes, such as the *quatrefoil* (Figure 6), cannot be obtained from the superellipse equation and the super-formula.

3. Results and Discussion

Figures 1-4 illustrate shapes that are created by varying the value of σ for $a=b=1$ and $\phi=0$ or $\pi/4$. Note that in Figure 1 and Figure 2, $\sigma \geq 0$ and that $-2<\sigma<0$ in Figure 3 and Figure 4.

As we can see in Figure 1, for $\sigma=0$, the graph is a rhombus with corners $(\pm a,0)$ and $(0,\pm b)$. This curve is the same as that obtained from the superellipse (see Equation (1)) with $n=1$. When σ is greater than 0, the sides of the curves become increasingly more concave as σ increases. In doing so, the curves associated with $\sigma>0$ behave similarly to those from the superellipse with $0<n<1$.

It can be verified that when $\sigma>0$ and $\phi=0$, our Cartesian Equation (19) defines closed and concave curves contained in the rectangle $-a\leq x\leq +a$ and $-b\leq y\leq +b$. When $-2<\sigma<0$ and $\phi=0$, the above equation generates closed but convex curves. In this case, the size of the region containing each curve depends on the value of σ. More precisely, we have $-A\leq x\leq A$ and $-B\leq y\leq B$ where $A=4a/\left(4-\sigma^2\right)$ and $B=4b/\left(4-\sigma^2\right)$ if $-2<\sigma<0$.

Although the above claims concerning boundedness, closure, convexity and concavity can be justified from the shapes generated by Equations (5) and (9), we present in that follows a brief derivation of the shape parameter and size of the region containing each curve when $a=b=1$ and $\sigma<0$. Taking account of the symmetry of our curves, it suffices to threat the case where $x\geq 0$ and $y\geq 0$ or, equivalently, $\cos\theta\geq 0$ and $\sin\theta\geq 0$ since $x=\rho\cos\theta$ and $y=\rho\sin\theta$. From Equations (6) and (9), we get

$$x=\frac{\cos\theta}{\cos\theta+\sin\theta+\sigma\sqrt{\cos\theta\sin\theta}} \tag{22}$$

since $\cos\theta\geq 0$ and $\sin\theta\geq 0$. Hence

$$\frac{\mathrm{d}x}{\mathrm{d}\theta}=-\frac{2\sqrt{\cos\theta\sin\theta}+\sigma\cos\theta}{2\sqrt{\cos\theta\sin\theta}\left(\cos\theta+\sin\theta+\sigma\sqrt{\cos\theta\sin\theta}\right)^2}. \tag{23}$$

It follows immediately from the above equation that $\frac{\mathrm{d}x}{\mathrm{d}\theta}=0$ yields

$$\sqrt{\cos\theta\sin\theta}=-\frac{\sigma}{2}\cos\theta \tag{24}$$

and then

$$\sin\theta=\frac{\sigma^2}{4}\cos\theta. \tag{25}$$

Substitution of Equations (24) and (25) into Equation (22) leads to

$$x_{\max}=\frac{\cos\theta}{\cos\theta+\frac{\sigma^2}{4}\cos\theta-\frac{\sigma^2}{2}} \tag{26}$$

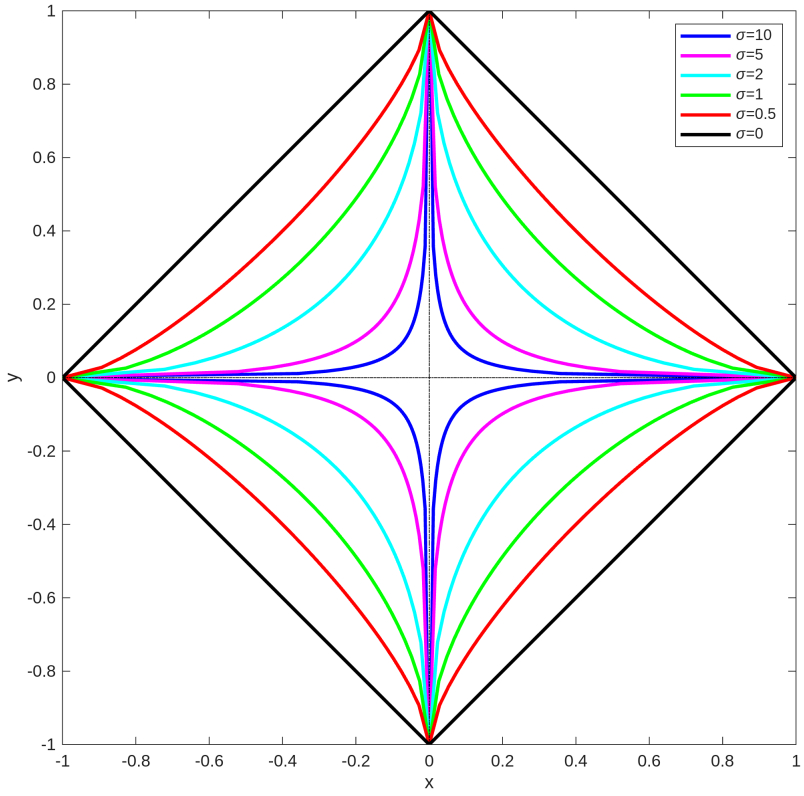


Figure 1. Shapes created by varying the value of σ with $\sigma \geq 0$ when $a = b = 1$ and $\phi = 0$.

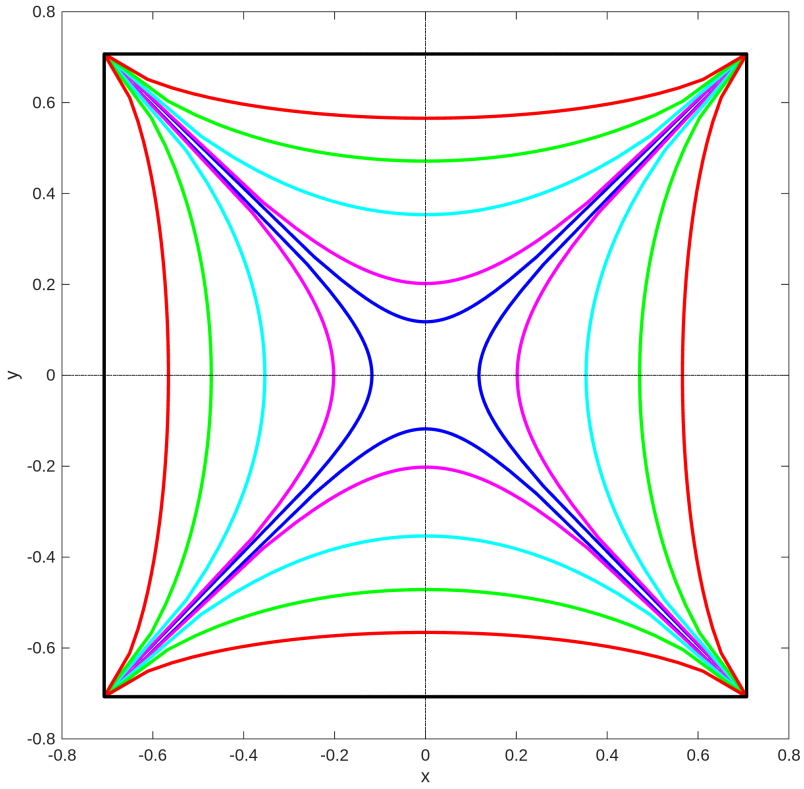


Figure 2. The same as **Figure 1** but with $\phi = \pi/4$.

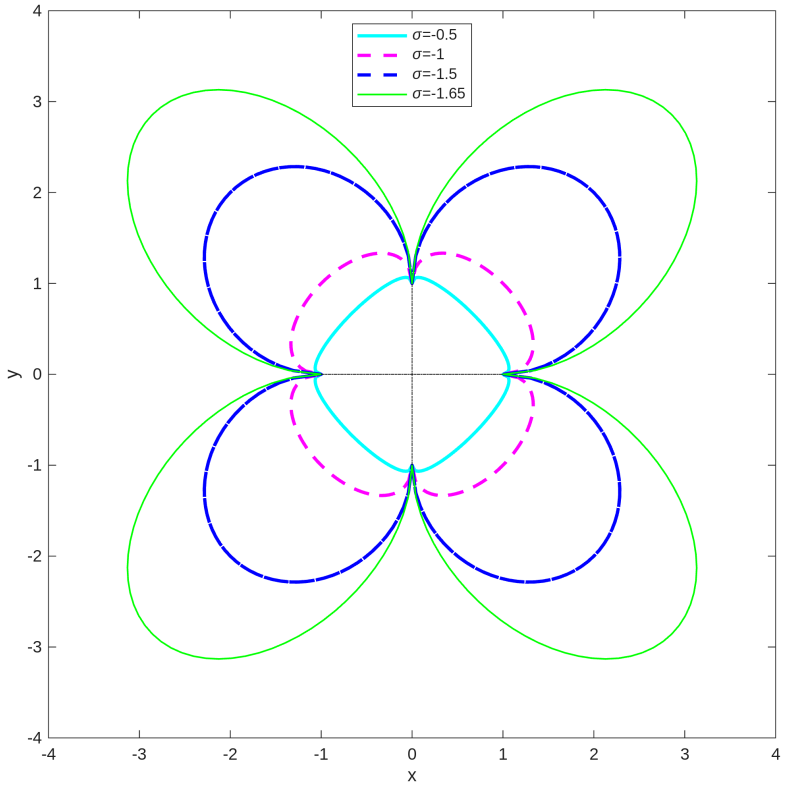


Figure 3. Shapes associated with four negative values of σ when $a=b=1$ and $\phi=0$.

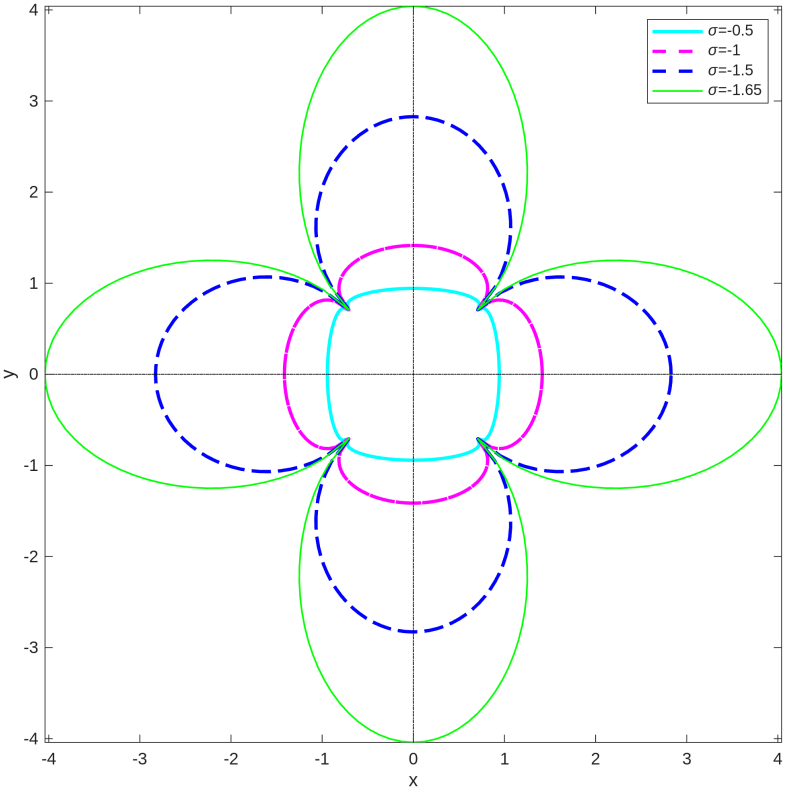


Figure 4. The same as **Figure 3** but with $\phi=\pi/4$.

or

$$x_{max} = \frac{4}{4-\sigma^2}, \tag{27}$$

which means that $-2 < \sigma < 0$ because $x \geq 0$ and $\sigma < 0$. Here, $x_{\max}$ refers to the maximum value of the abscissa x. Consequently,

$$-4/\left(4-\sigma^2\right) \leq x \leq 4/\left(4-\sigma^2\right), \ -2 < \sigma < 0 \tag{28}$$

given the symmetry of our curves. In the same way, we got the same result for the y coordinate:

$$-4/\left(4-\sigma^2\right) \leq y \leq 4/\left(4-\sigma^2\right), \ -2 < \sigma < 0. \tag{29}$$

When $(a,b) \neq (1,1)$, we obtain

$$-4a/\left(4-\sigma^2\right) \leq x \leq 4a/\left(4-\sigma^2\right), \ -2 < \sigma < 0 \tag{30}$$

and

$$-4b/\left(4-\sigma^2\right) \leq y \leq 4b/\left(4-\sigma^2\right) \tag{31}$$

because the transition from $a = b = 1$ to $(a,b) \neq (1,1)$ corresponds to the non-linear scaling given by Equation (10).

Let us indicate that when $\sigma > 0$, the radius vector ρ is such that $0 < \rho < 1$, which implies that $-a \leq x \leq a$ and $-b \leq y \leq b$.

In Figure 5 (resp. Figure 6), we show the shape associated with $\sigma = \sqrt{2}$ (resp. $\sigma = -\sqrt{2}$). Figure 6 has the form of a *quatrefoil*. By plotting the two graphs on the same axes, we obtain Figure 7.

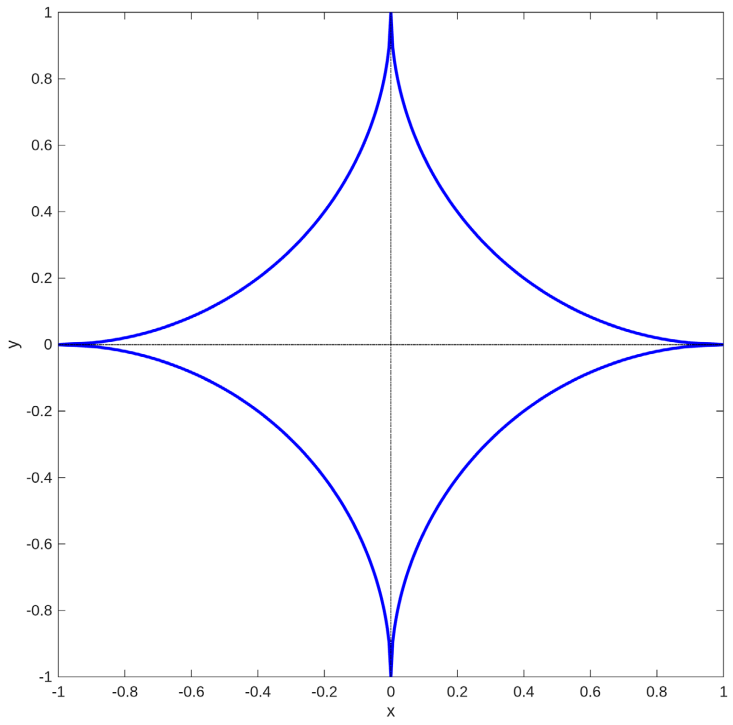


Figure 5. Shape associated with $\sigma = \sqrt{2}$ when $a = b = 1$ and $\phi = 0$.

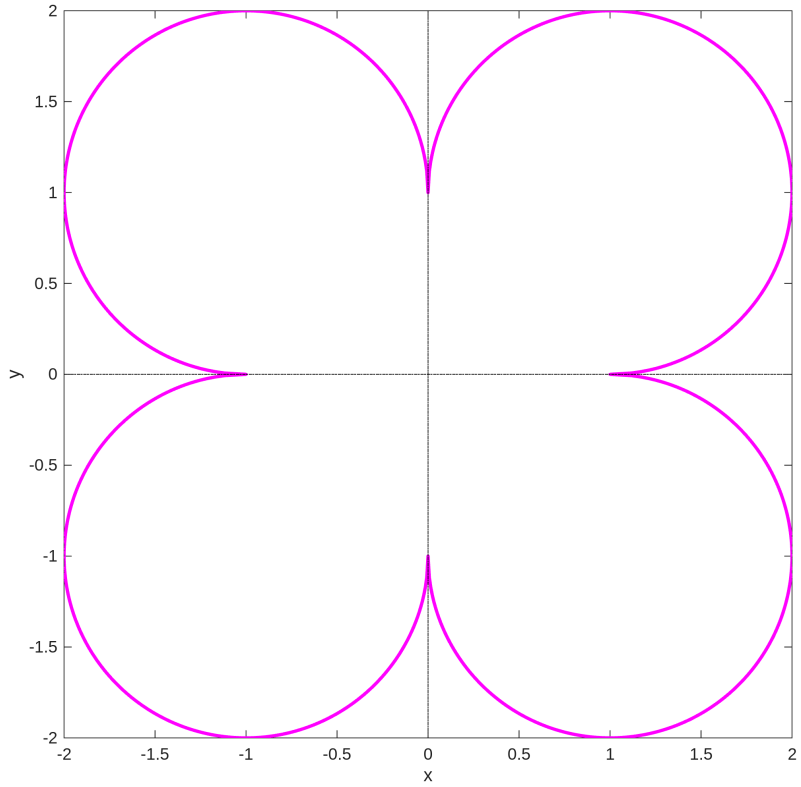


Figure 6. Shape associated with $\sigma = -\sqrt{2}$ when $a = b = 1$ and $\phi = 0$.

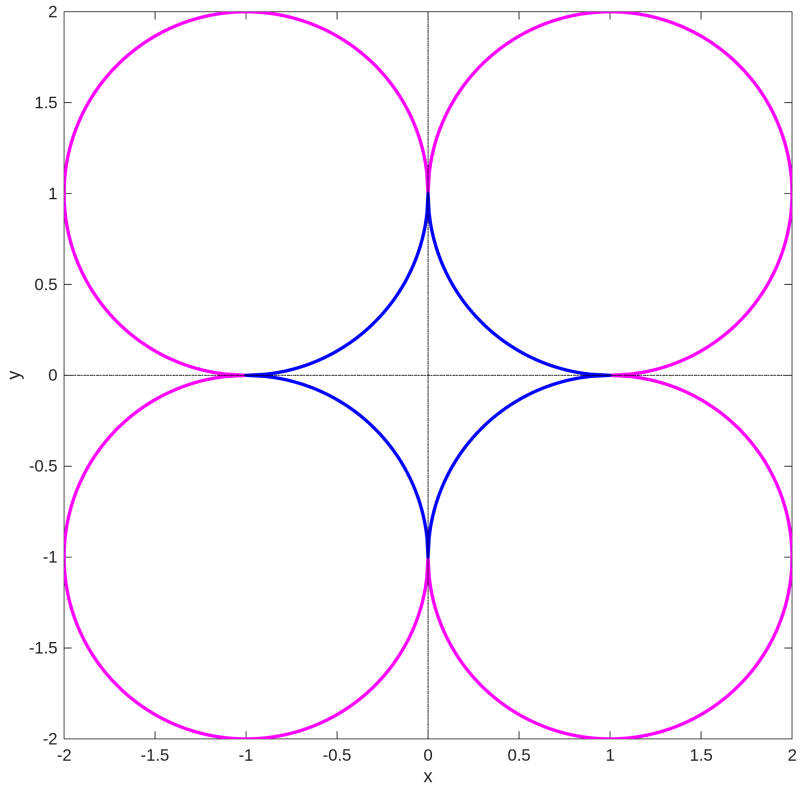


Figure 7. Shapes created with $\sigma = -\sqrt{2}$ (magenta color) and $\sigma = \sqrt{2}$ (blue color) in the same Cartesian coordinate system when $a = b = 1$ and $\phi = 0$.

Figure 8 and Figure 9 show some shapes resulting from adding Equations (5) and (15) side by side for several values of the parameter σ ($\sqrt{2}$, 0.5, 0, −1, $-\sqrt{2}$ and −1.75). This combination yields a doubling of the number of sides, but also the modification of their shapes.

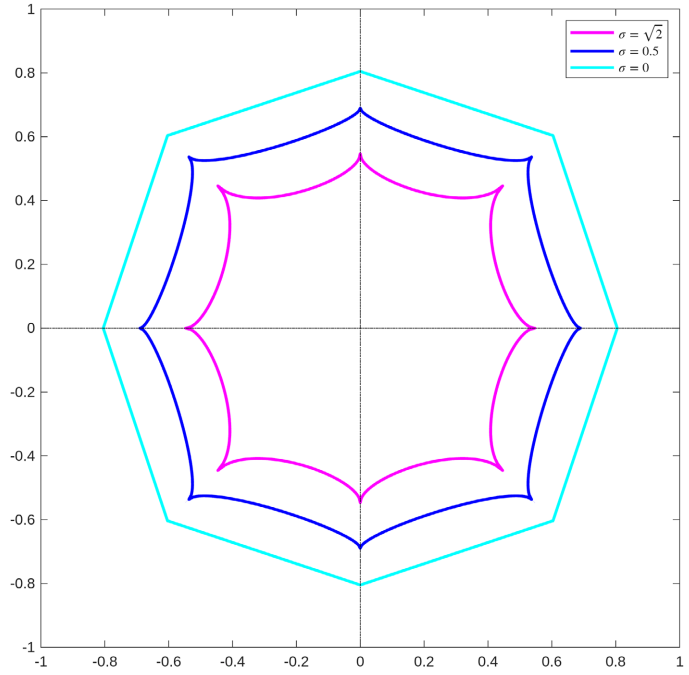


Figure 8. Shapes created with the combination of Equations (5) and (15) for three positive values of the parameter σ.

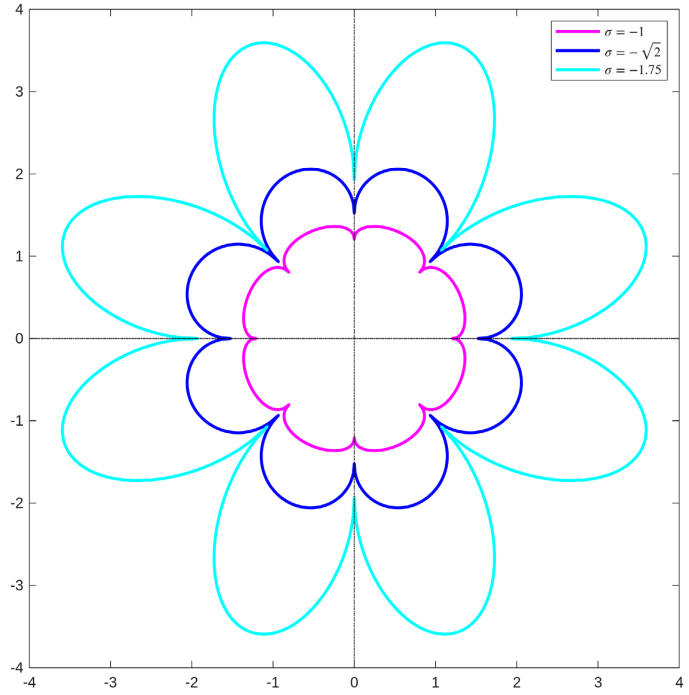


Figure 9. Shapes created with the combination of Equations (5) and (15) for three negative values of the parameter σ.

In Figure 10 and Figure 11, examples are shown of shapes generated by Equations (17) and (18). It is easy to observe that these shapes are notably different from those already encountered in this work.

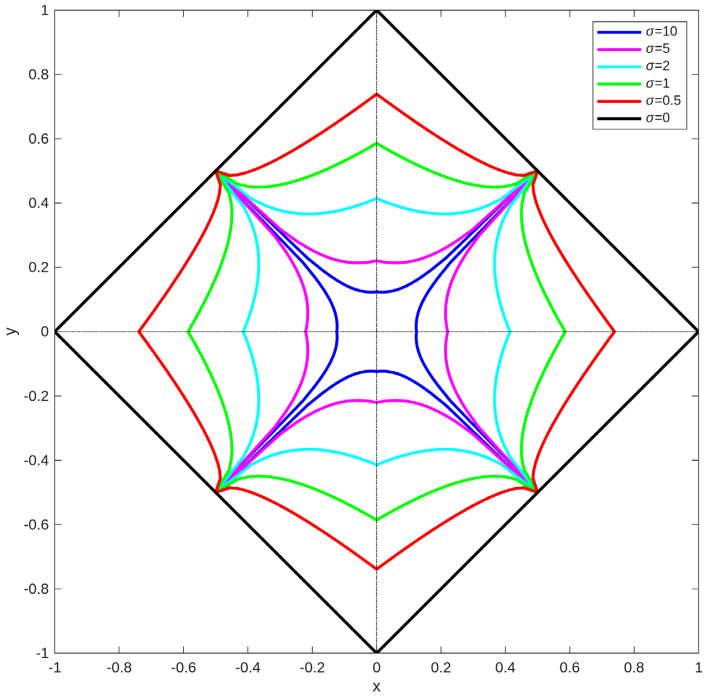


Figure 10. Shapes generated by Equations (17) for several non-negative values of the parameter σ.

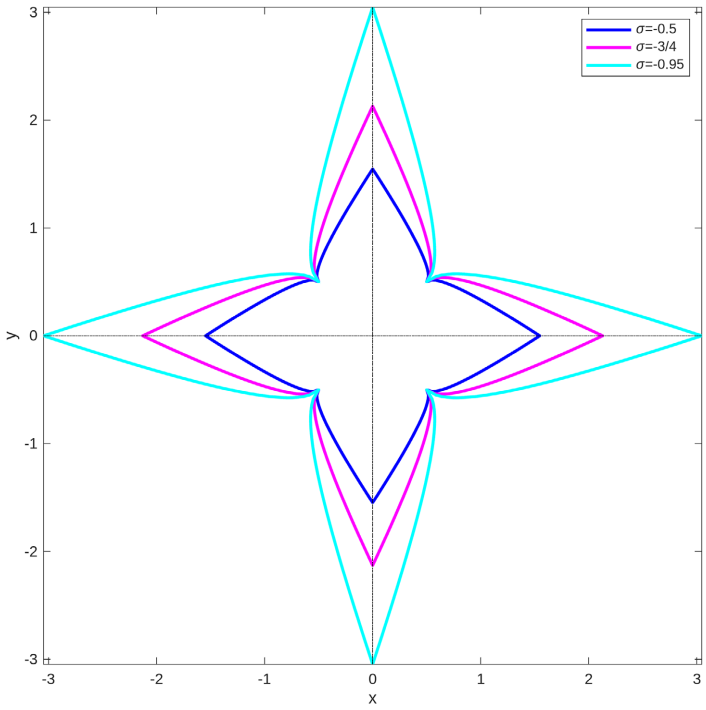


Figure 11. The same as Figure 10 but with three negative values of the parameter σ.

Before finishing this section, we have to indicate that multiplication (side by side) of the two equations obtained from Equation (11) by choosing $\sigma = \pm\sqrt{2}$ yealds the ellipse of equation

$$\left|\frac{x}{a}\right|^2 + \left|\frac{y}{b}\right|^2 = 1 \tag{32}$$

which becomes a circle of radius a centered at the origin of a Cartesian coordinate system having X and Y as axis lines if $a = b$. Furthermore, Equations (9), (12), (14), (16) and (20) modify the behavior of functions and then the shapes of associated graphs. These equations can be considered as modifications of a constant function $R = 1$ (deformation of the unit circle), as shown in **Figure 12**, but other functions $f(\theta)$, such as trigonometric functions, can be used as well. **Figure 13** (resp. **Figure 14**) shows the graph of $\rho(\theta)\cos(\theta)$ and $\rho(\theta)\sin(\theta)$ with $\rho(\theta)$ given by Equation (9), $\sigma = -1.5$ and $\phi = 0$ (resp. $\phi = \pi/4$).

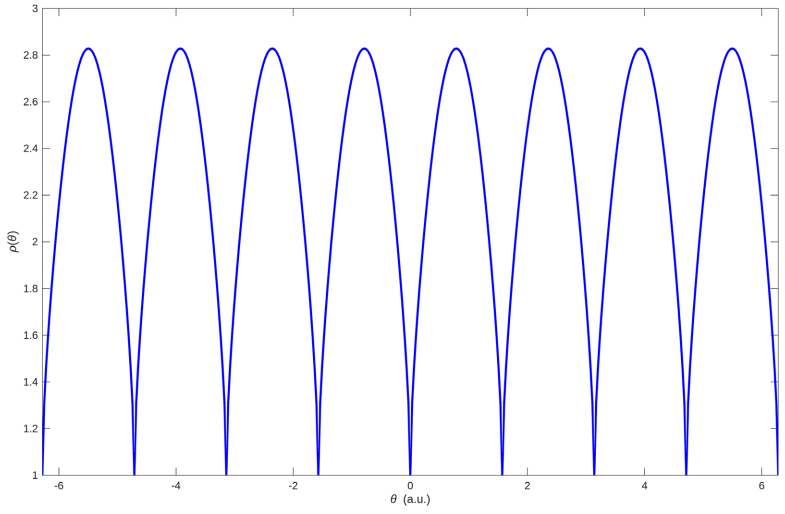


Figure 12. Plot of $\rho(\theta)$ for $\sigma = -1.5$ and $\rho(\theta)$ defined by Equation (9).

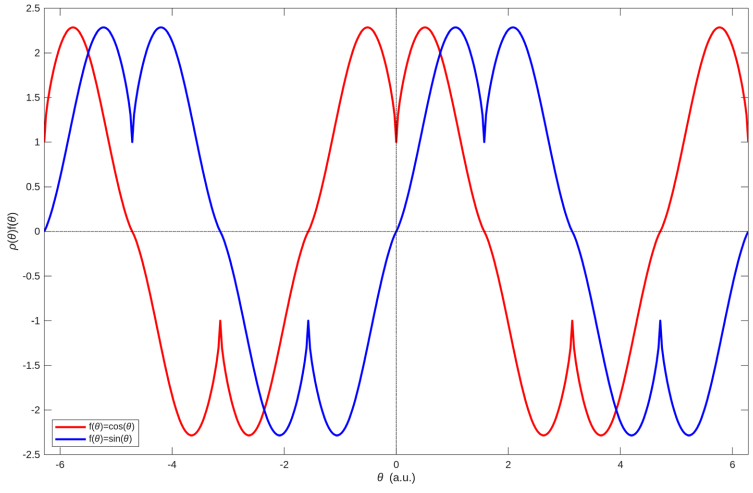


Figure 13. Plots of $\rho(\theta)\cos(\theta)$ and $\rho(\theta)\sin(\theta)$ for $\sigma = -1.5$, $\phi = 0$ and $\rho(\theta)$ defined by Equation (9).

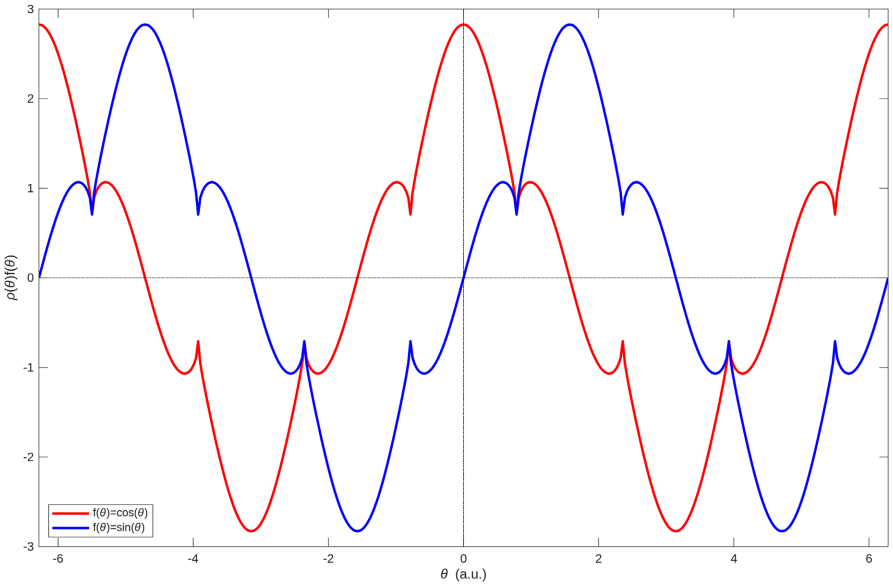


Figure 14. The same as **Figure 13** but with $\phi = \pi/4$.

4. Conclusion

As described herein-above, the formulas established in this work can yield a wide range of geometric shapes and forms among which the rhombus, several concave and convex closed curves with four or eight sides, the circle, the ellipse, and so on. We have shown that applying a polar equation to a constant function or other functions such as the cosine and sine functions modifies the behavior of these functions and then the shapes of the associated graphs. We hope that our formulas have the potential to transform the way we look at geometric shapes and forms in a profound manner.

Author Contributions

Salomon Mboninyibuka formulated ideas, goals and aims. He also performed writing-original draft. Hippolyte Nyengeri performed supervision, visualization and writing-review & editing.

Conflicts of Interest

The authors declare no conflicts of interest.

References

[1] Gielis, J. (2003) A Generic Geometric Transformation that Unifies a Wide Range of Natural and Abstract Shapes. *American Journal of Botany*, **90**, 333-338. https://doi.org/10.3732/ajb.90.3.333

[2] Giels, J.L.A. (1999) US7620527B1-Method and Apparatus for Synthesizing and Analyzing Patterns Utilizing Novel "Super-formula" Operator. https://patents.google.com/patent/US7620527B1/en

[3] Wikipedia Superellipse. https://en.wikipedia.org/wiki/Superellipse

[4] Superellipse (Lamé Curve). https://fractional-calculus.com/super_ellipse.pdf

[5] Spíchal, L. (2019) Modeling the Cross-Sectional Shape of the Long Bones Using the Superellipse. In: Bastinec, J. and Hrubý, M., Eds., *Proceedings of the International Conference of Mathematics, Information Technologies and Applied Sciences* 2019, University of Defense, 2019.

[6] Gridgeman, N.T. (1970) Lamé Ovals. *The Mathematical Gazette*, **54**, 31-37. https://doi.org/10.2307/3613154

[7] Masaya, M. (2014) Asymptotic Behaviour of the Maximum Curvature of Lamé Curves. *Journal of Geometry and Graphics*, **18**, 45-59.

[8] Gardner, M. (1965) Mathematical Games. *Scientific American*, **213**, 222-236. https://doi.org/10.1038/scientificamerican0965-222

[9] Lamé, G. (1818) Examen des différentes méthodes employées pour résoudre les problèmes de géométrie. Mme Ve Courcier.